Interlaboratory Round Robin Study on Axial Tensile Properties of SiC/SiC Tubes*

G. Singh^{a†}, S. Gonczy^b, C. Deck^c, E. Lara-Curzio^a and Y. Katoh^a

^aOak Ridge National Laboratory, Oak Ridge TN, USA ^bGateway Materials Technology, Inc., Mt. Prospect, IL, USA ^cGeneral Atomics Inc., San Diego, CA, USA

Abstract Continuous SiC fiber-reinforced SiC matrix (SiC/SiC) composite is one of the candidate materials for accident tolerant fuel cladding systems due to its high temperature stability, chemical inertness and stability under neutron irradiation. An extensive statistical database on the mechanical properties of SiC/SiC composite is much needed to estimate the failure probability in evolving thermomechanical conditions as well as for the rigorous analysis of the material's behavior under normal and off-normal reactor conditions. In addition to the properties database, test standards, which ensure the reliable, unbiased characterization of the material, are needed. The mechanical properties database, particularly for tubular SiC/SiC specimens, is limited and new standardized test methods are still under development. With the objective of expanding the database of mechanical properties of nuclear grade SiC/SiC and establishing the precision and bias statement for ASTM C1773 standard, an interlaboratory round-robin study was conducted on the tensile strength of SiC/SiC tubes at room temperature. The mechanical properties statistics from the round robin study and the precision statistics and precision statement are presented herein. The data show reasonable consistency across the laboratories, indicating that the current C1773-13 ASTM standard is adequate for testing ceramic fiber reinforced ceramic matrix composite tube specimens. Limited statistical variation in the mechanical properties show that the quality of the SiC/SiC material employed in these tests is adequate for meeting the nuclear applications. The ultimate tensile strength data seems to follow the Weibull distribution and the proportional limit strength data fit best with the lognormal distribution, for the tested SiC/SiC composite material.

Keywords: SiC, composite, axial, tensile, precision and bias, round robin, nuclear, cladding

1. INTRODUCTION

Background and Objectives

Silicon carbide (SiC) fiber-reinforced SiC matrix composites (SiC/SiC composites) offer a set of properties that make these materials highly suitable for many high temperature applications. Like monolithic SiC ceramics SiC/SiC composites maintain their mechanical properties and chemical inertness even at temperatures beyond the upper limit for typical metallic superalloys. These composite materials

1

^{*} This manuscript has been authored by UT-Battelle, LLC under Contract No. DE-AC05-00OR22725 with the U.S. Department of Energy. The United States Government retains and the publisher, by accepting the article for publication, acknowledges that the United States Government retains a non-exclusive, paid-up, irrevocable, world-wide license to publish or reproduce the published form of this manuscript, or allow others to do so, for United States Government purposes. The Department of Energy will provide public access to these results of federally sponsored research in accordance with the DOE Public Access Plan (http://energy.gov/downloads/doe-public-access-plan).

[†] Corresponding author: singhgp@ornl.gov

have high specific strength and reasonable damage tolerance. Some of the applications for which SiC/SiC composites are being considered include heat exchangers, reformers, reactors and filters in chemical industry, preheaters, recuperators and radiation tubes in heat transfer systems, space vehicles, furnace components combustion and turbine sections of gas turbine engines and nuclear reactors.

The Fukushima Daiichi nuclear power plant accident led to wide spread safety concerns over existing nuclear reactors around the globe. In efforts to enhance the safety of nuclear power plants extensive research and development work on improving the accident tolerance of fuel-cladding systems is being conducted [1, 2]. Because of the stability of SiC/SiC composites under neutron irradiation conditions, low activation and other properties as mentioned above, SiC/SiC is a promising candidate material for the accident tolerant fuel cladding systems in light water reactors (LWR) [3, 4]. It should be noted here that the stability under irradiation is a unique property of SiC/SiC composite in the class of composite materials and is not offered by other composites including carbon fiber based composites. Besides application in LWRs, SiC/SiC composites have has potential structural and insulation applications in other nuclear energy systems, such as Very High Temperature Reactor (VHTR) [5, 6], Gas-Cooled Fast Reactor (GFR) [7], Molten Salt Reactor (MSR), sodium fast reactor (SFR), and fusion reactors [8, 9]. Although SiC/SiC composites are manufactured in the forms of chopped fiber composites, particulate-reinforced composites and continuous fiber composites, only continuous fiber SiC/SiC composites are suitable for fuel cladding fabrication.

Although SiC/SiC composites are promising materials for cladding and core components of nuclear reactors, several design considerations and critical engineering issues need to be addressed before the material can be deployed and commercialized [10]. A "qualified" database of properties of SiC/SiC composite will be needed for performing rigorous experimental and numerical studies to determine the viability of the material for specific applications. In general, a "qualified" database is one which is generated using procedures which comply with standards associated with the design code of the component of interest. In the absence of a qualified database, the studies for assessment of the material either cannot be carried out or the results of the studies cannot be interpreted and applied with confidence, leading to designs with high safety margins. Besides, the designer cannot use a material (without a database) directly in new designs but has to 1) provide evidence that the material complies with the code requirement and 2) obtain permission to use that material in design [11]. Thus, lack of a comprehensive property database can significantly hamper the development of the technology and can negatively affect the material development.

Nuclear grade SiC/SiC composite consists of near-stoichiometric and crystalline beta-phase SiC for both fibers and matrix, and less-radiation-stable interphase which is the material between the fibers and matrix. The current database of mechanical properties for nuclear grade SiC/SiC composite is limited. Although various properties of nuclear grade SiC/SiC composites were previously measured, tube specimens were not used in these studies [12]. Most of the studies utilized rectangular bars and disc specimens for thermo-mechanical and physical property evaluations. The ASTM standard test methods for axial tensile test (ASTM C1773-13) and hoop tensile test (ASTM C1819-15) of continuous-fiber reinforced ceramic composite tubes have been developed and become available only recently. However, these two ASTM standards lack the precision and bias statements which convey important information to the users of the ASTM standard about the practical applicability of their test results. In other words, these standards need round-robin studies to develop precision and bias statements.

Several studies [13-17] have been conducted in the past to evaluate the properties of SiC/SiC composites. Nozawa et al. [13] conducted tensile and compressive tests on flat specimens of three types of composites: plain-weave CVI, plain-weave NITE and unidirectional NITE SiC/SiC composites. It was found that for tensile loading, Young's modulus, proportional limit stress (PLS) and fracture strength

decreased with increase in the angle between the fiber orientation and the load direction, while the Poisson's ratio increased. The study also demonstrated that the Tsai-Wu [14] criterion can model the effect of anisotropy on the in-plane tensile and compressive stresses. In another study, Rohmer et al. [15] conducted axial and hoop tensile tests on CVI SiC/SiC tube specimens which had fiber braids oriented at ±30° with the tube axis. The axial tensile strength (463 MPa) and axial PLS (82 MPa) were found to be much greater than the hoop tensile strength (63 MPa) and hoop PLS (36 MPa). The axial and hoop Young's moduli were reported to be 232 GPa and 158 GPa, respectively. Both the studies by Nozawa et al. [13] and Rohmer et al. [15] demonstrated the strong influence of fiber orientation on the mechanical properties of SiC/SiC composite. Deck et al. [16] conducted hoop tensile tests and uniaxial tensile tests on CVI SiC/SiC composites. Hoop test were conducted through C-ring tests as well as expanding plug tests. The study involved hoop biased (fiber reinforcement greater in hoop direction by 1.5:1 ratio), axial biased (1.3:1) and unbiased tube specimens. The reported results show a significant effect of biasing on the Young's modulus and strength properties of the material. Bernachy-Barbe et al. [17] conducted several mechanical tests and reported modulus, tensile, compressive and shear strength data for CVI SiC/SiC specimens. Although these studies have contributed data on the SiC/SiC composite mechanical properties, the database is still far from being comprehensive.

The current work described in this paper aims to fill these gaps in the development process of SiC nuclear fuel cladding technology. An interlaboratory round robin study on the tensile properties of SiC/SiC tubes was conducted involving several different laboratories from government institutions, academia and industry. This interlaboratory study served multiple objectives: 1) Expand the limited database of mechanical properties of SiC/SiC composite and 2) Develop precision statement for the ASTM C1773 Standard Test Method (Monotonic Axial Tensile Behavior of Continuous Fiber-Reinforced Advanced Ceramic Tubular Test Specimens at Ambient Temperature).

Precision & Bias of a Test Standard

Currently few standards exist for mechanical testing of continuous fiber-reinforced ceramic matrix composites (CMC) at ambient temperature. Of these standards, American Society for Testing and Materials (ASTM) standards are widely accepted and used. This is partly because the ASTM standards include precision and bias statements which are lacking in other standardized test methods. However, the current ASTM standards on mechanical testing of CMCs (ASTM C1773-13, ASTM C1819-15) do not include these statements due to the nature of the material and lack of wide data base on a variety of advanced ceramic composite tubes tested in tension. The work presented herein focuses on determining the precision and bias for this test standard.

Test Procedure

These objectives were accomplished through the interlaboratory round robin study which was conducted according to the ASTM E691-09 standard: Standard Practice for Conducting an Interlaboratory Study to Determine the Precision of a Test Method. Primary mechanical properties of interest are axial elastic modulus, axial proportional limit stress and the corresponding strain, ultimate tensile strength and the corresponding strain. As a first step ORNL performed the lead test to identify the difficulties and issues with the testing of the SiC/SiC tube specimens. The test protocol was prepared addressing the difficulties identified in the lead test. The findings from the lead test were also discussed with the specimen provider General Atomics, and the specimen design was modified accordingly. The objective of the test protocol was to help the interlaboratory participants to rigorously implement the ASTM C1773-13

requirements and fulfill the specific requirements pertaining to the testing of the SiC/SiC tube specimens employed in this study. After the completion of the ORNL lead test, the specimens, fixtures and other parts for testing were distributed to the interlaboratory study participants. The participating laboratories independently tested the specimens according to the test protocol and reported the test results in a set duration of time.

2. TEST MATERIAL

Nuclear Grade SiC/SiC Composite

In this study 47 nuclear grade SiC/SiC composite specimens were tested by seven laboratories for tensile properties at room temperature. The data from 43 specimens were used for calculating the statistics; 4 specimens could not be successfully tested. The tube specimens were specifically designed for the interlaboratory round robin testing. These tube specimens were made of nuclear grade SiC/SiC composite material; the constituents were CVI SiC matrix, Hi-Nicalon Type S fibers and pyrocarbon interphase fiber coating, all of which are stable under the neutron irradiation. In addition to the material constituents, the fiber architecture and the associated properties were selected such that the specimens represented a typical accident tolerant fuel cladding. The strength degradation of the SiC/SiC composite material by irradiation occurs only at high doses [18]. The swelling and change in the thermal conductivity of the SiC/SiC composite saturates at about 1 dpa [18]. The typical properties of SiC/SiC composite tube specimens are listed in Table 1. Figure 1 shows the porous microstructure and non-circularity in the cross-section of a SiC/SiC tube specimen.

Table 1: Typical properties of SiC/SiC composite tube specimens at room temperature. Source [12, 15-17, 19-22]

Property	Value
Density	$2.3 - 2.8 \text{ g/cm}^3$
Porosity	10 – 20%
Fiber volume fraction	30 – 40%
Young's modulus	170 – 250 GPa (tensile) 250 GPa (compressive)
Shear modulus	80 – 120 GPa reported for flat specimens
Poisson's ratio	~0.13 for 0°/90°, ~0.25 for ±45° (in-plane) for flat specimens
Proportional limit stress	80 – 110 MPa (axial) 100 – 160 MPa (hoop)
Ultimate tensile strength	230 – 270 MPa (axial) 200 – 340 MPa (hoop)

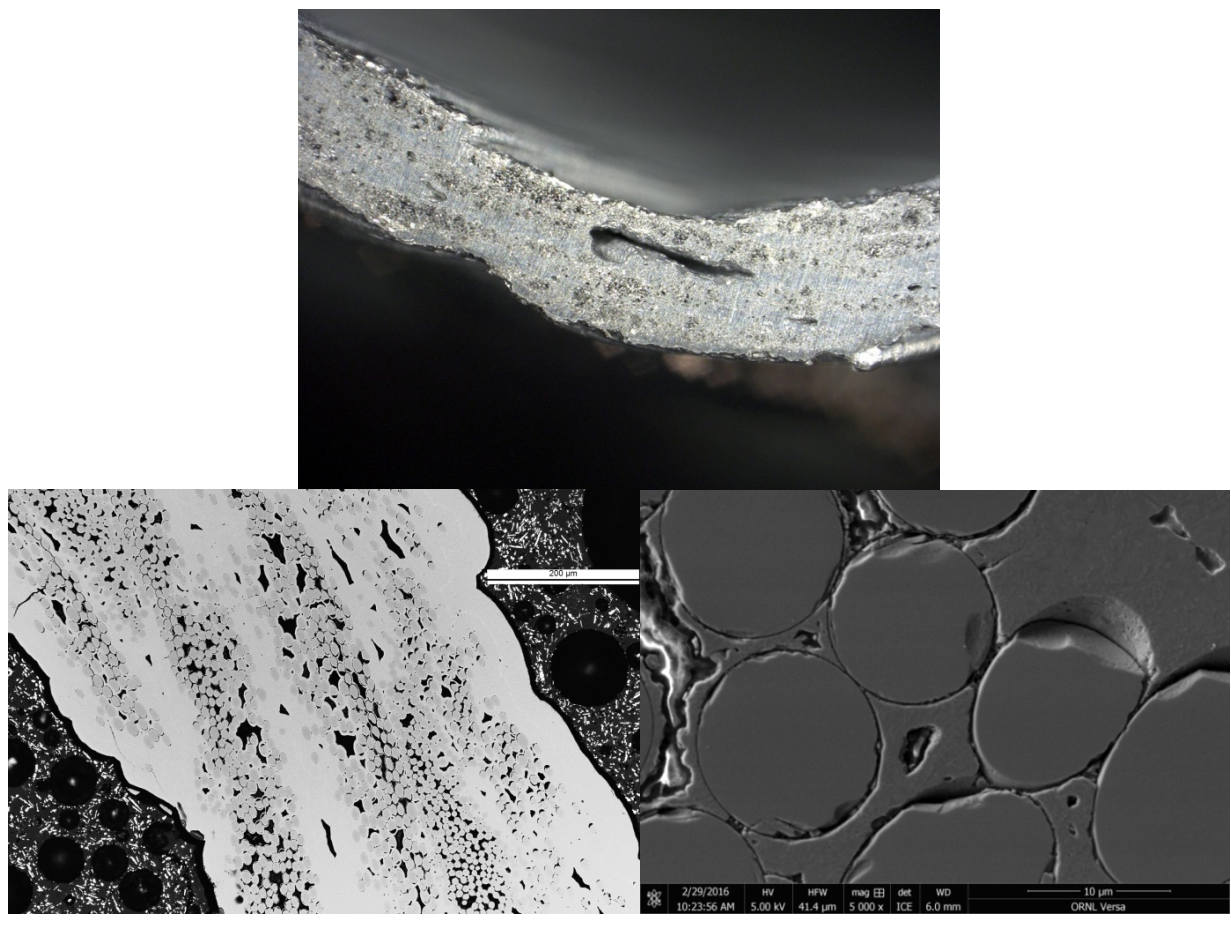


Figure 1: Cross-sectional planes of a SiC/SiC tube as observed by optical microscopy (top, lower left) and scanning electron microscopy (lower right).

2.1 FIBER, MATRIX, AND INTERPHASE

Fiber

The SiC/SiC composite used for this study contains Hi-NicalonTM Type S fibers. These fibers are near stoichiometric (manufacturer-claimed C/Si atomic ratio of ~1.05), stable under neutron irradiation, show limited irradiation creep [23] and can maintain thermal creep strength up to 1400°C [24]. The fibers have a typical chemical composition of Si:C:O as 69:31:0.2 wt% and the tensile strength and tensile modulus are 2.6 GPa and 420 GPa, respectively [25, 26]. The typical filament diameter and density are 11μ and 3.10 g/cc. These fibers are commercially produced by NGS Advanced Fibers Co. (Toyama, Japan). Extensive research efforts on the development of these fibers are presented in reference [27].

Interphase

A 150nm monolayer of pyrocarbon (PyC) forms the interphase coating between the fiber and matrix in the SiC/SiC composite used for this work. The interphase coating plays an important role in imparting mechanical properties to SiC/SiC composites; interphase material is weaker and more compliant than both fiber and matrix, and it deflects cracks propagating through the matrix, thus preventing fiber cracking and breakage. The interphase coating imparts pseudo ductility to the composite material by

allowing the fibers to debond and slide and to bridge matrix cracks. For nuclear applications only PyC or PyC/SiC are suitable choices [28].

Matrix

The composite material used in this interlaboratory study has high-purity SiC matrix. Similarly, to the fibers, only near stoichiometric matrices with high crystallinity and a minimum of secondary phases are stable in irradiation environments. Of the several techniques available to densify the matrix, CVI has been found to produce a SiC matrix of the required quality [29]. Besides, the Nano-Infiltration and Transient Eutectic-Phase (NITE) process has also been found to produce SiC/SiC composites that are stable under irradiation [30-32]. The CVI process was used in this work to prepare the SiC/SiC specimens.

2.2 REINFORCEMENT AND ARCHITECTURE

Silicon carbide fibers are typically produced as single multifilament tows. These tows are then weaved or knitted to form a variety of fabric types, including preforms. Preforms are a type of fabric form suited for a particular application in terms of shape, mechanical and structural requirements. Fiber preforms for the test material were fabricated using triaxial braiding. This weaving style allows the fabric to conform to complex shapes and retains balance on both side of the fabric. The fiber tow bundles were stacked in $\pm 55^{\circ}$ orientation with some fiber bundles at 0° direction for axial reinforcement. This type of stacking imparts symmetric in-plane strength to the material.

An axial tensile test specimen is shown in Figure 2. The specimens are 150 mm in length with 8° tapered shoulders. The nominal wall thickness, outer diameter and gage section length are 0.8 mm, 9.5 mm and 70 mm respectively. Figure 2 shows the steel end plugs bonded into the shoulder sections that prevent crushing in the grip fixtures.



Figure 2: An axial tensile test specimen with steel end plugs.

3. TEST METHOD

3.1 DIMENSIONAL MEASUREMENT USING RADIOGRAPHY

The dimensions of all the specimens (outer and inner diameters) were measured at ORNL using radiography. The accuracy of the measurements was ± 0.02 mm. The radiography images for each specimen were taken at three angles 0° , 60° and 120° as shown in Figure 3. For each image the dimensions were measured at three different locations along the gage length. The outer and inner

diameters were calculated as the average of these 9 measurements. The wall thickness of the specimen was calculated from the average outer and inner diameters. The average outer diameter, inner diameter and wall thickness for all the specimens were measured to be 9.53 mm, 7.97 mm and 0.78 mm respectively. The standard deviation in the OD, ID and wall thickness of all the specimen were 0.062 mm, 0.060 mm and 0.027 mm, respectively.

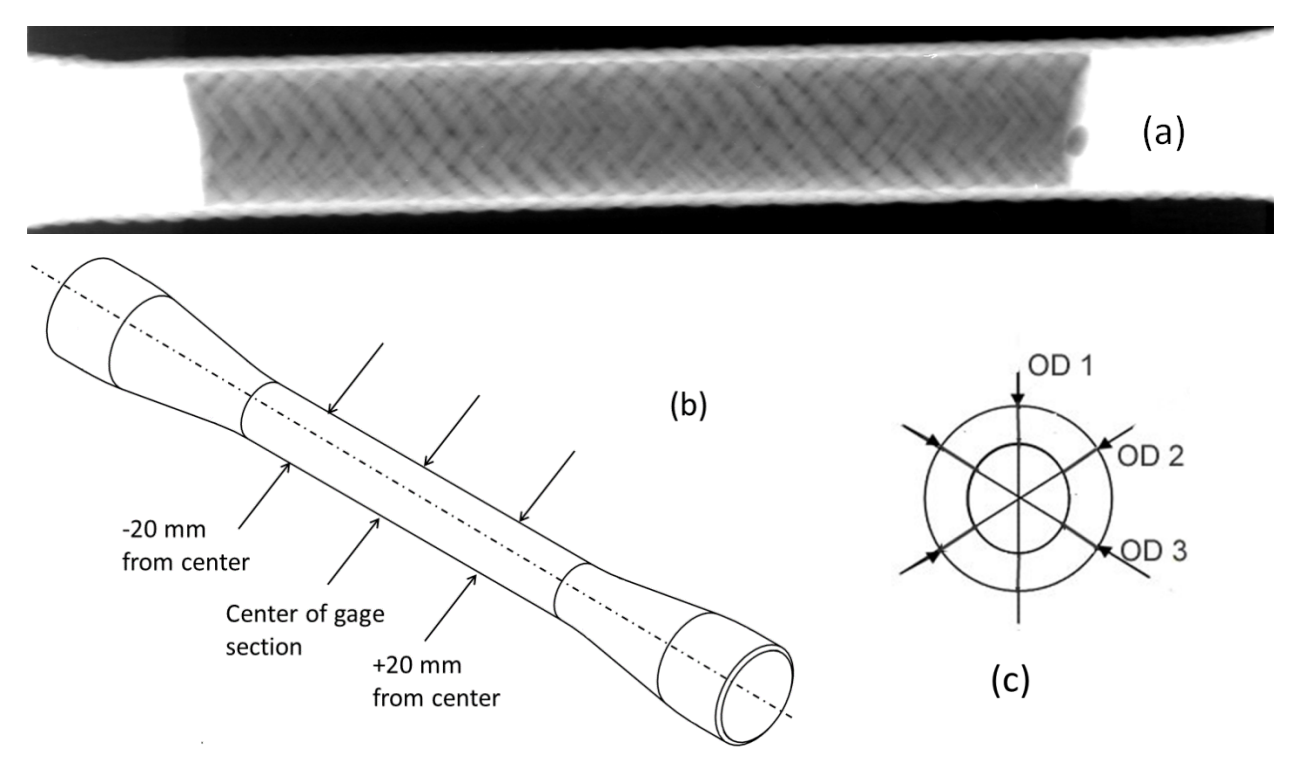


Figure 3: Radiography image of a tensile test specimen (a); locations for dimension measurement (outer and inner diameters) along the gage length (b) and angular locations for dimension measurement (c).

3.2 TEST PROCEDURE

3.2.1 Grip Fixtures

There are two types of grip fixtures that are commonly used for testing CMC specimens with the tube geometry: active and passive. The passive grip fixtures do not require a direct application of gripping force; rather, the axial force applied by the test machine is employed to generated compressive force on the fixture either through adhesive bond or by mechanical features in the grips. For this work passive grip fixtures were used. Figure 4 shows the fixture employed for gripping the tube specimens. The test specimen is directly in contact with the copper collets (see Figure 5) which served the dual function of holding the specimen inside the fixture and also minimizing the bending in the specimen by deforming and realigning itself in response to the bending moment. The specimens had adhesively bonded steel end plugs to prevent crushing in the grip sections of the test specimen, as shown in Figure 2.

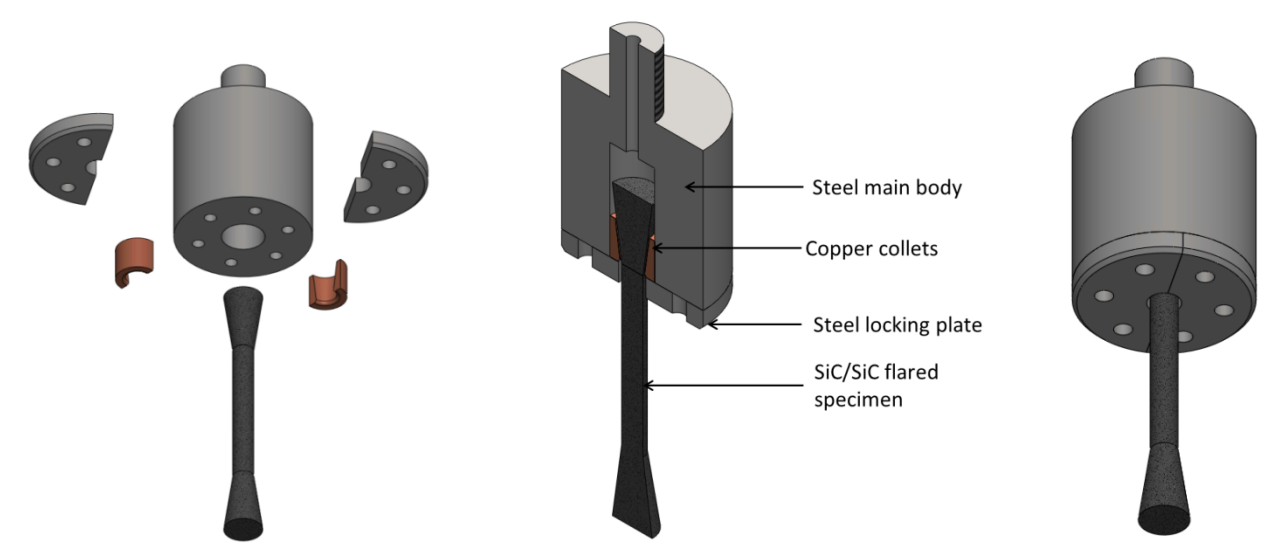


Figure 4: Passive fixture for gripping the specimen during the axial tensile tests.



Figure 5: Annealed copper collets with tapered inner surface

3.2.2 Test Protocol and ASTM C1773-13 Standard

The standard test method ASTM C1773-13 (Standard Test Method for Monotonic Axial Tensile Behavior of Continuous Fiber-Reinforced Advanced Ceramic Tubular Test Specimens at Ambient Temperature) was used to conduct the axial tensile test on SiC/SiC tubular specimens.

Prior to the test the top and bottom fixtures were aligned to reduce the bending. In addition, swivel joints were used to minimize the bending that is introduced by the deviations in the specimen geometry from the nominal dimension (see Figure 6).



Figure 6: Swivel joints employed to minimize the bending which occurs due to irregular geometry of the specimen.

Unlike their monolith counterparts, which undergo catastrophic fracture, continuous fiber-reinforced ceramic matrix composite (CMC) accumulate damage during the loading process. Due to the gradual damage process, CMCs exhibit a non-linear stress-strain behavior after the elastic limit. (See Figure 15) So, displacement controlled tests were employed to prevent "run away" condition – a rapid uncontrolled deformation and fracture. The test machine was set up for an initial cross-head position, zero load, and displacement mode and a displacement rate of 0.76 mm/min. The specimens were preloaded to 7-9 lb. The strain was measured with extensometer. Figure 7 shows a specimen while being tested in the Oak Ridge National Laboratory test rig. Acoustic sensors were used to understand the progressive damage in the SiC/SiC specimen.



Figure 7: A specimen in the ORNL test rig.

4. RESULTS

4.1 MEASURED PROPERTIES AND DISTRIBUTION FIT

Because of the nature of the round robin the confidentiality of the identities of the participating organizations is preserved. Table 2 below lists the data for ultimate tensile strength (UTS), proportional limit stress (PLS), Young's modulus, strain at failure and strain at proportional limit stress. For comparing across laboratories, strength and strain data are shown in figures 8 and 9 respectively. Figures 10 and 11 show the fit of several probability distributions to the global UTS and PLS data sets respectively.

The UTS was found to be consistent across the specimens with the small coefficient of variance (COV) of 12.5%. As can be noted from Figure 8, the laboratory means ranged from 220 to 257 MPa; the small range indicates consistency across the laboratories. However, the COVs for individual laboratories ranged from 5.5% to 19.8% indicating significant variation in the with-in lab spread of the UTS data across the seven laboratories. Thus, the test operator and the test equipment can significantly contribute to the variation in the UTS property of SiC/SiC material. From the goodness of fit test (see Figure 10 and Table 3) it can be inferred that UTS data fit best with the 2-parameter Weibull distribution. The shape and scale parameters for the Weibull distribution fit were calculated to be 10.1 and 249.1.

The all laboratory mean for PLS was found to be 92.6 MPa with COV of 9.7% indicating consistency in the PLS property across the specimens. The laboratory means ranged from 79.8 MPa to 97.6 MPa as shown in Figure 8. The with-in lab COVs for PLS ranged from 6.3% to 13.4%. Except for Lab3 COVs were under 10% indicating a high consistency in the PLS property within and across the

laboratories. As can be noted from Table 3, the goodness of fit test showed that the Lognormal distribution fits best the PLS data with the log mean and log standard deviation as 4.52 and 0.096.

The all laboratory mean for Young's modulus was found to be 202.7 GPa with COV of 19.9%. The laboratory mean varied for 146.5 MPa to 240.4 MPa and the COV ranged from 6.0% to 22.6%. A large variation in the mean may be due to the due to inconsistency in the method of calculating modulus from the stress-strain data. A relevant discussion is presented in section 5.2.

Table 2: Results from the interlaboratory round robin axial tensile testing of SiC/SiC tubes.

		Ultimate Tensile Strength (MPa)		Limi			oung's lus (GPa)			Strain at Proportional Limit Stress (%)	
	Test Count	Mean	COV(%)	Mean	COV(%)	Mean	COV(%)	Mean	COV(%)	Mean	COV(%)
Lab1	5	220.0	12.6	95.9	9.5	210.8	16.2	0.46	17.9	0.056	6.6
Lab2	7	245.6	6.0	85.6	9.1	191.4	6.0	0.57	8.5	0.056	8.8
Lab3	6	256.7	6.5	79.8	13.4	146.5	9.2	0.63	7.5	0.059	10.7
Lab4	6	220.8	19.8	99.8	9.0	232.4	13.5	0.46	28.2	0.063	15.4
Lab5	7	233.2	19.4	91.2	9.8	202.4	9.7	0.52	26.7	0.055	8.9
Lab6	5	242.6	5.5	93.8	6.6	189.7	22.6	0.53	8.9	0.055	11.3
Lab7	7	236.2	8.0	97.6	6.3	240.4	17.8	0.53	9.9	0.052	13.0
All Labs	43	236.8	12.5	92.6	9.7	202.7	19.9	0.53	18.5	0.057	12.0
Labs Sta	tistics*	236.4	5.6	92.0	7.7	201.9	15.4	0.52	8.5	0.057	6.1

^{*}For Labs Statistics row, Mean represents the mean of the laboratory means, COV represents the coefficient of variance of the laboratory means.

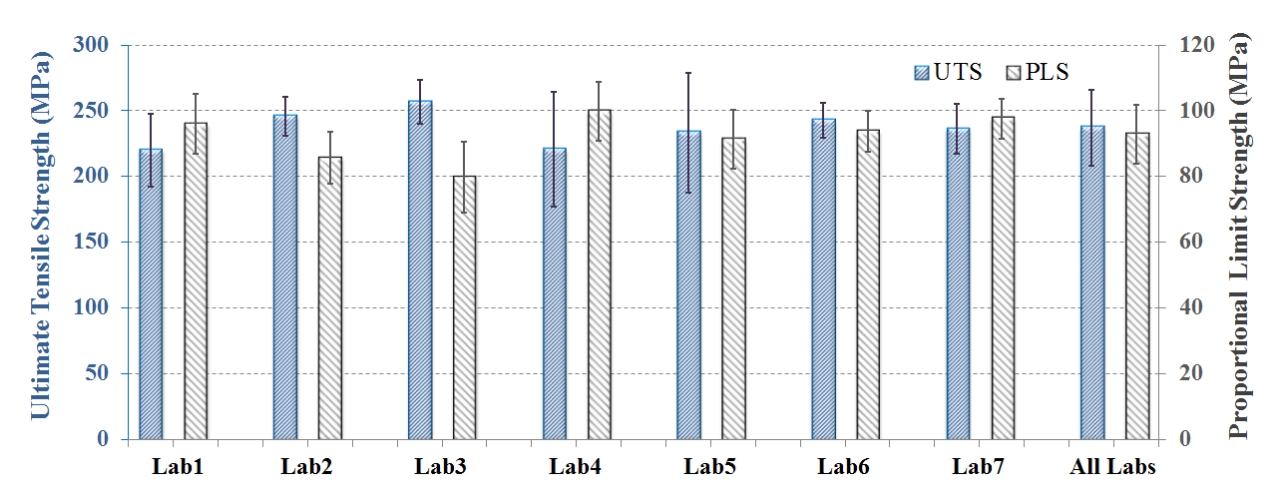


Figure 8: Ultimate tensile strength (UTS) and proportional limit stress (PLS) for each laboratory obtained from interlaboratory round robin testing (Error bar: ±1 S.D.).

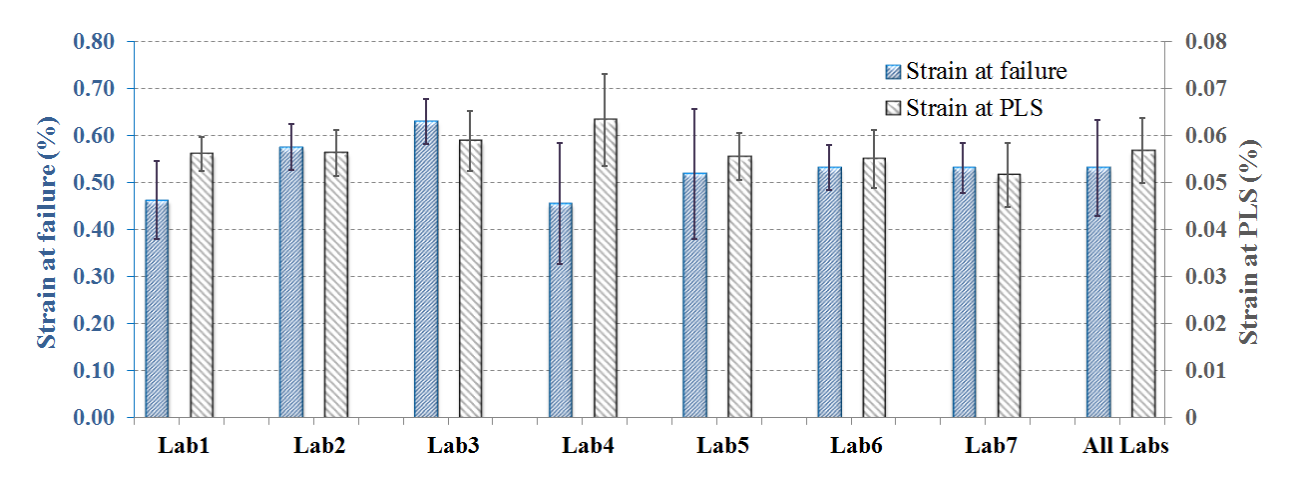


Figure 9: Strain at failure and strain at proportional limit stress (PLS) for each laboratory obtained from interlaboratory round robin testing (Error bar: ±1 S.D.).

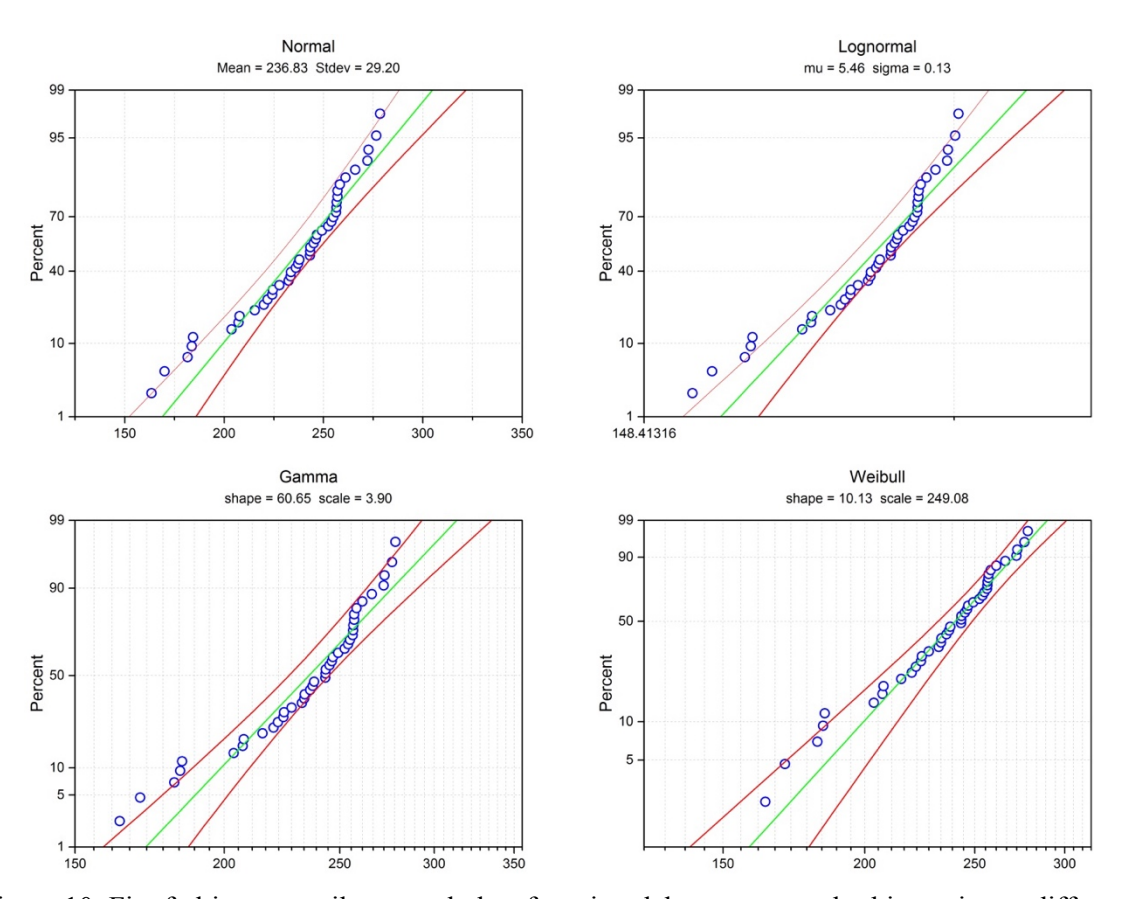


Figure 10: Fit of ultimate tensile strength data from interlaboratory round robin testing to different probability distribution functions, with 95% confidence bound lines

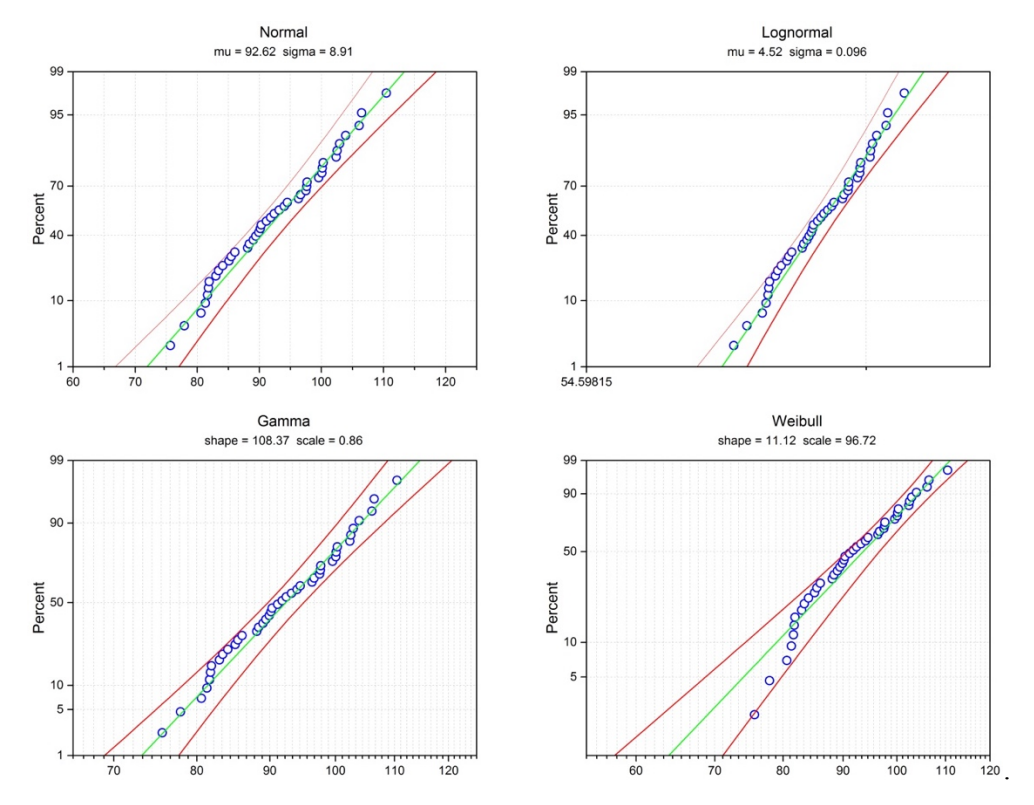


Figure 11: Fit of proportional limit stress data from interlaboratory round robin testing to different probability distribution functions.

Table 3: Goodness of fit statistics for each distribution fit to the strength data.

Lower statistics indicate a better fit.

	Distribution	Statistics				
Ultimate	Normal	0.097				
tensile strength	Lognormal	0.119				
	Weibull	0.074				
	Gamma	0.110				
	Normal	0.072				
Proportional	Lognormal	0.065				
limit stress	Weibull	0.092				
	Gamma	0.068				

Figures 12 and 13 show the 95% confidence bounds for the UTS and PLS data fit to Weibull and Lognormal distributions respectively. For individual laboratories, the confidence bounds are significantly larger than the confidence bound for all laboratories data, due to the small number of specimens per lab (5-7). However, fair overlapping of confidence bounds indicates similar data statistics for the laboratories. For PLS the confidence bounds overlap well indicating very similar statistics for PLS across the laboratories. The confidence bounds for all laboratories data are also shown in the figures.

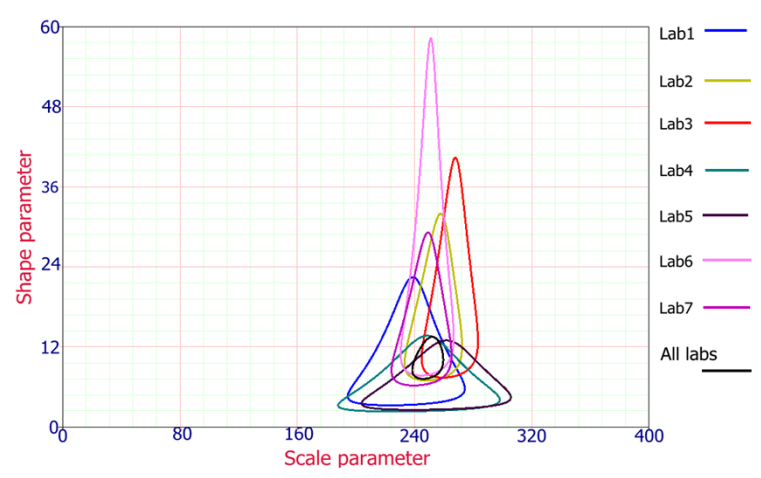


Figure 12: Weibull distribution based 95% confidence bounds for ultimate tensile strength.

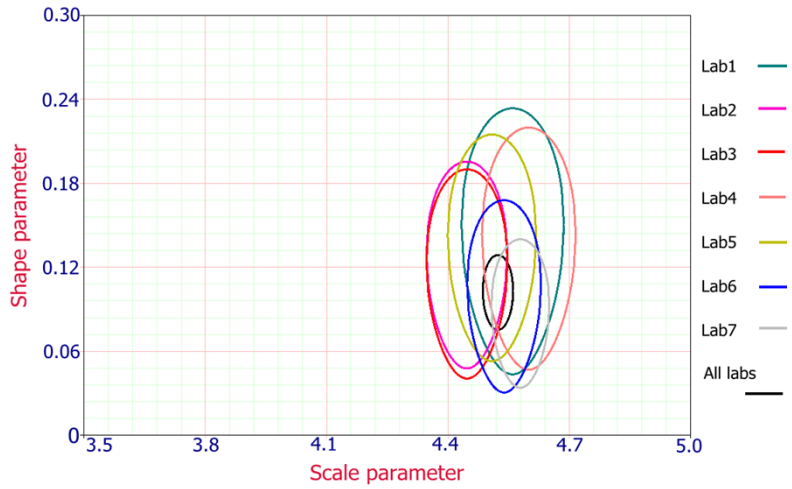


Figure 13: Lognormal distribution based 95% confidence bounds for proportional limit stress.

4.2 PRECISION AND BIAS STATEMENTS

Precision

When specimens of a presumably identical material are tested under presumably identical conditions within and between laboratories, the test data often have significant statistical variation. Apart from the random variation in the material itself, operators, test equipment and environmental factors also contribute to the variation in the test results. If the tests are conducted over a larger span of time then the variation in the results is usually greater. The differences in calibration of the equipment can contribute to variability in the test results. Thus, there are many factors which lead to variability in the results and these factors vary within a given laboratory and also between laboratories. It is important to take into account

the variability caused due to these factors before the test data can be used for any particular application. For instance, if two materials A and B are compared for tensile strength and the values obtained for material A are higher, then it may be not because material A is stronger than material B but it could be due to variability in the test conditions.

The closeness of the test result to the accepted reference value is generally termed as accuracy. The standard test methods report this accuracy in terms of precision and bias. The ASTM definition of precision is the closeness of agreement between independent test results on the same property of identical test material, expressed in terms of *repeatability* and *reproducibility*. Repeatability refers to the accuracy and random variability of the results obtained with the same method on identical test items in the same laboratory by the same operator using the same equipment within short intervals of time within a single laboratory. Reproducibility refers to the accuracy and random variability associated with successive measurements of the same property carried out by operators working in different laboratories, each obtaining single results on identical test material when applying the same method Thus, precision of a test method provides an estimate of the variation the user of the test method can expect, which in turn reflects the utility of the standard test method. The ASTM definition of bias is the difference between the expectation of the test results and an accepted reference value

The precision statistics were calculated from the round robin data in accordance with ASTM E691-09 standard. The precision statement for this study is stated below:

An interlaboratory test program gave the following precision statistics for the most commonly measured tensile properties of a CMC (SiC/SiC with HNLS fiber, CVI SiC matrix, PyC interphase) tube with nominal fiber volume fraction of 51%, an average bulk density of 2.71 g/cm³, and an average open porosity of 14%.

Table 4: Precision statistics calculated from the interlaboratory round robin data.

Mechanical Property	$\overline{\mathbf{x}}$	$\mathbf{s}_{\mathbf{x}}$	$\mathbf{s_r}$	$\mathbf{s}_{\mathbf{R}}$	r	R
UTS (MPa)	236.4623	13.2751	28.7144	29.7146	80.4	83.2
PLS (MPa)	91.9774	7.0779	8.4193	10.5288	23.6	29.5
Young's modulus (GPa)	201.9270	31.1474	30.5109	42.0486	85.4	117.7
Strain at failure (%)	0.5286	0.0608	0.0862	0.1003	0.24	0.28
Strain at PLS (%)	0.0566	0.0036	0.0063	0.0069	0.02	0.02

 $[\]overline{\mathbf{x}}$: mean of the laboratory means

No statement of bias can be made because no acceptable standard reference material exists for the SiC-SiC tube material.

5. DISCUSSION

5.1 EFFECT OF DIMENSION MEASUREMENT TECHNIQUE ON STATISTICS

Since, the dimensional measurement of the specimens is an integral part of calculating the mechanical properties, accurate measurement of dimensions is very important. The roughness of the composite surface makes it difficult to measure external dimensions accurately. Therefore, the dimensions of the specimen used in this study were measured using radiography, as discussed in section 3.1. However, for the purpose of highlighting the influence of dimension measurement technique on the evaluated properties, a comparison was performed for a laboratory (Lab5) data. The data is for 7 specimens. In addition to radiography, the dimensions were also measured with a Vernier caliper. Some

s: standard deviation of laboratory means

s_.: repeatability standard deviation

 $[\]mathbf{s}_{\mathbf{R}}$: reproducibility standard deviation

r: 95% repeatability limit (within laboratory) for 7 laboratories and 5-7 tests for each laboratory

R: 95% reproducibility limit (between laboratories) for 7 laboratories and 43 tests

of the specimens, which failed in the cylindrical-to-conical transition region, were sectioned after the test to measure the dimensions. Since the failure strain of this material is very small ($\sim 0.5\%$) it is reasonable to assume that the dimension after the test is same as that before the test.

The outer diameter and wall-thickness were measured at three different locations along the gage length; at each location measurements were made at angles 0°, 60° and 120° as described in section 3.1 for radiography technique. The cross-sectional area was calculated using the mean outer diameter and wall thickness obtained from the nine measurements for each specimen. Table 5 shows the dimensions measured by the radiography and caliper. As can be noted from the table, the difference in the wall thickness measurement leads to significant difference in the cross-sectional area: area calculated using caliper is over 15% greater than the area measured using radiography. The properties evaluated using both the dimensions were compared. Table 6 shows the evaluated properties. The mean cross-sectional area of the specimens measured by the two methods differs by 18%. As can be noted from Table 6 the difference in UTS, PLS and Young's modulus based on the two dimensions is over 15% indicating a strong influence of the dimension measurement technique on the calculated properties statistics.

Table 5: Comparison of dimensions of SiC/SiC tube specimens measured using radiography and vernier caliper.

P	Outer dia	meter (mm)	Wall thick	ness (mm)	Cross-sectional area (mm²)		
	Mean	COV	Mean	COV	Mean	COV	
Radiography	9.51	0.50	0.78	3.94	21.41	3.61	
Caliper	9.73	0.78	0.90	3.77	25.26	3.54	
Difference in mean (%)	2.3		13	3.3	15.2		

Table 6: Comparison of properties evaluated using radiography and caliper based dimensions for laboratory Lab5.

aboratory Labs.								
	Cross-sectional area (mm²)		Ultimate tensile strength (MPa)		Proportional limit stress (MPa)		Young's modulus (GPa)	
	Mean	S.D.	Mean	S.D.	Mean	S.D.	Mean	S.D.
Radiography based dimensions	21.41	0.77	233.2	45.3	91.2	9.0	202.4	19.6
Caliper based dimensions	25.26	0.89	198.0	40.5	77.2	6.4	171.3	13.7
Difference in mean (%)	-18.0		15.1		15.4		15.4	

The reason for difference in the measurement of cross-sectional area for the two methods is shown in Figure 14. The wall-thickness measured by the caliper is greater than that measured by the radiography. The dimensions measured by the radiography are based on the image analysis and the distance between the two surfaces can be directly measured by calculating the pixel and calibrating the pixels to real length. Thus, the limitations imposed by the surface roughness of the specimen are not applicable for the radiography technique. For the same reason the dimensions measured by microcomputed tomography are expected to be more accurate than that measured using mechanical instrument such as caliper or micrometer.

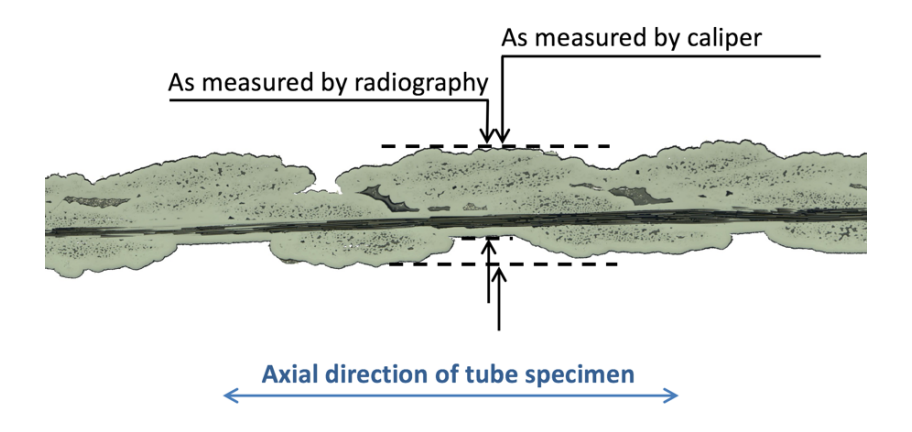


Figure 14: Measurements on a specimen wall; the surface roughness of the composite specimen leads to inaccurate measurement of the wall thickness by caliper, compared to radiography.

5.2 METHOD FOR MEASURING YOUNG'S MODULUS

It was noted that the analysis method significantly influences the value of Young's modulus. The stress-strain data from Lab3 was analyzed in two ways: (1) Lab3 calculated the Young's modulus considering data in 0.01 - 0.04% strain range 2) ORNL recalculated Young's modulus considering data in 0.005 - 0.04% strain range. In the both the calculations, a line was linearly fit to the stress-strain data. The Young's modulus determined by ORNL was about 18% higher than that determined and reported by the Lab3. The significant difference in the Young's moduli independently determined by the laboratories highlights the importance of standardizing the procedure for calculating Young's modulus. A procedure below is proposed for calculating the Young's modulus and proportional limit stress.

Perhaps the maximum contribution to variation in the determined Young's modulus across different laboratories comes from the difference in the region of the stress-strain curve which is selected to determine the Young's modulus. Therefore, to have consistency in the procedure employed for calculating the modulus, the strain range should be defined instead of selecting it arbitrarily. For defining this strain range these steps can be followed (see Figure 15): first the slope of the stress-strain curve should be evaluated for the entire linear strain range, when the slope of stress-strain curve is plotted against strain, the highest region of the curve, where the slope is maximum, is taken as the strain range for calculating the Young's modulus. The upper and lower limit of this range can be defined based on the allowed variability in the proportional limit stress that these limits will introduce. A linear fit is made to the data in this strain range. The slope of the linear fit is the Young's modulus of the specimen. From the lowest point of this range a line is extended down to the strain axis with its slope as the modulus. The intercept of this extended line with the strain axis is intercept A. The stress-strain curve is then shifted left by distance A. The proportional limit stress is determined based on the shifted stress-strain curve using the appropriate offset which will vary from material to material.

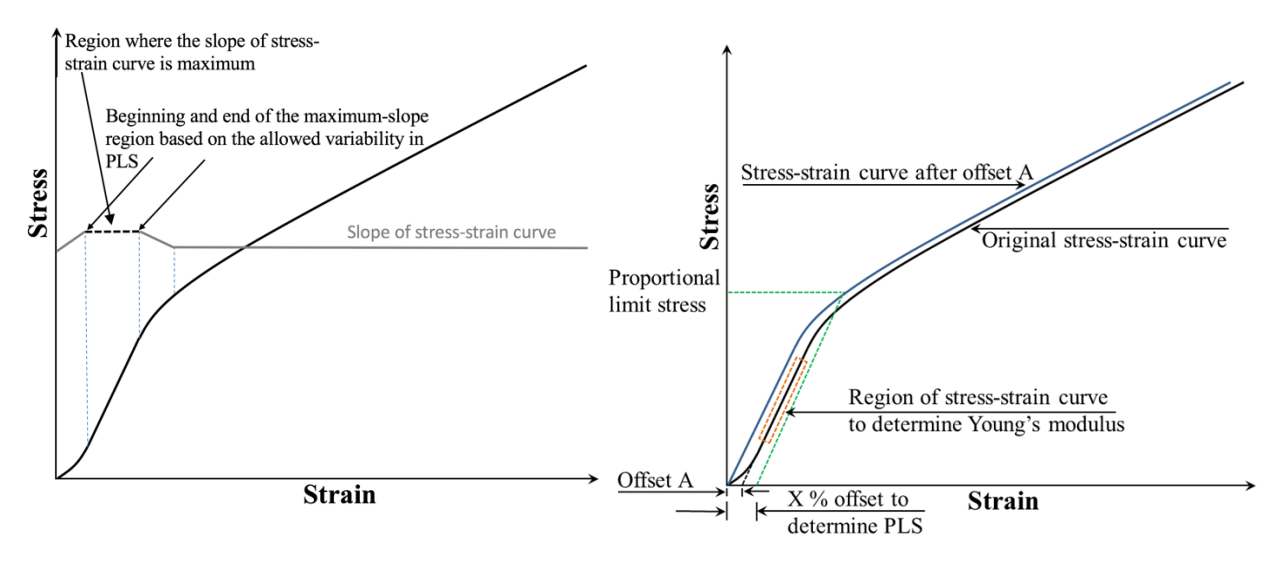


Figure 15: Proposed method to determine the Young's modulus and proportional limit stress.

5.3 TRANSITION SECTION FAILURES VS MID-GAGE SECTION FAILURES

Test specimens failed in the mid-gage section as well as in the transition section as shown in Figure 16. Here the transition section refers to the section where the straight cylindrical gage region transitions into the conical grip section of the specimen. Ideally the specimen should fail in the mid-region of the straight cylindrical section, but 33 of 43 specimens failed in the transition section. A comparison of the statistics was made to understand if the properties statistics for the specimens that failed in transition section are different from the statistics for specimens that failed in mid-gage section. Table 7 shows the comparison of the statistics. As can be noted from Table 7, the differences in the mean values are less than 8% for all the properties. The strain at PLS is same for both the failure types; the difference in PLS and strain at failure is less than 2%; the difference in UTS is less than 5% and for Young's modulus the difference is less than 8%. The same strain at PLS, and small differences in other properties indicate that the effect of failure locations had negligible effect on the mechanical properties.



Figure 16: Specimens with failure in transition section (leftmost specimen) and mid-gage section.

Table 7: Comparison of the material properties obtained from the specimens that failed in the mid-gage section and transition section.

	Test Count	Ultimate tensile strength (MPa)		Proportional limit stress (MPa)		Young's modulus (GPa)		Strain at failure (%)		Strain at PLS (%)		
		Mean	S.D.	Mean	S.D.	Mean	S.D.	Mean	S.D.	Mean	S.D.	
Mid-gage section failures	10	229.6	21.9	91.3	7.8	191.2	41.4	0.52	0.08	0.057	0.004	
Transition section failures	33	239.0	31.4	93.0	9.4	206.1	39.9	0.53	0.10	0.057	0.007	
Difference in mean %		-4.	-4.1		-1.9		-7.8		-1.9		0	

5.4 FAILURE MODE

A typical stress-strain curve obtained from the tests is shown in Figure 17. The stress-strain curve for composites essentially has three regions: 1) initial linear region which has highest slope, 2) the midregion which is curved and the slope reduces continuously in this region and 3) the linear region at the end. When the specimen is initially loaded in tension the load is shared by the both the fibers and matrix. This loading range constitutes the first region of the stress-strain curve. The matrix, being weaker than the fibers, starts microcracking (at the strain of about 0.0005 for the specimens used in the present study). With increasing applied force, load damage accumulates in the matrix, the cracks start propagating and run into the interphase which deflects the cracks around the fibers. Cracking of the interphase leads to debonding of fibers from the matrix. This loading range where matrix damage is accumulating constitutes the second region of the stress-strain curve. Since the damaged matrix is not able to sustain the load, the entire load is transferred to the fibers. In this loading range, which constitutes the third part of the stress-strain curve, slope angle is smaller than that in the first region of the curve and it remains practically constant in the third section of the stress-stain slope. Figure 18 shows the fiber pull-out in the tested specimen indicating a high toughness non-brittle failure mode with the typical composite failure.

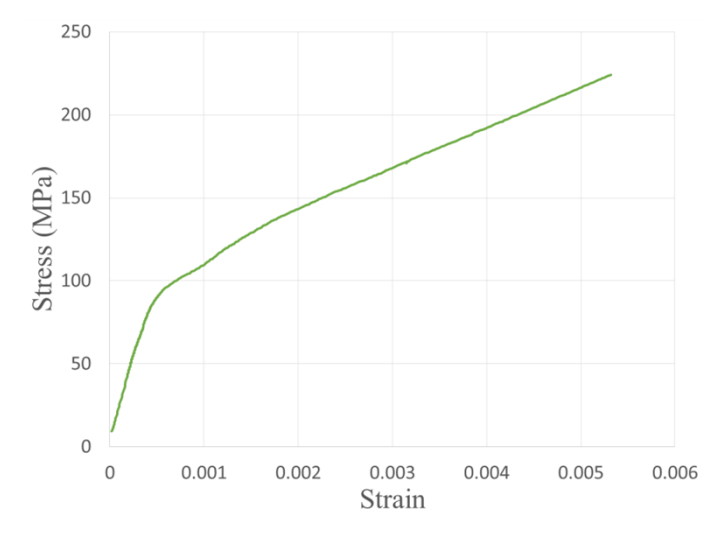


Figure 17: A typical tensile stress-strain curve obtained from the round robin tests.

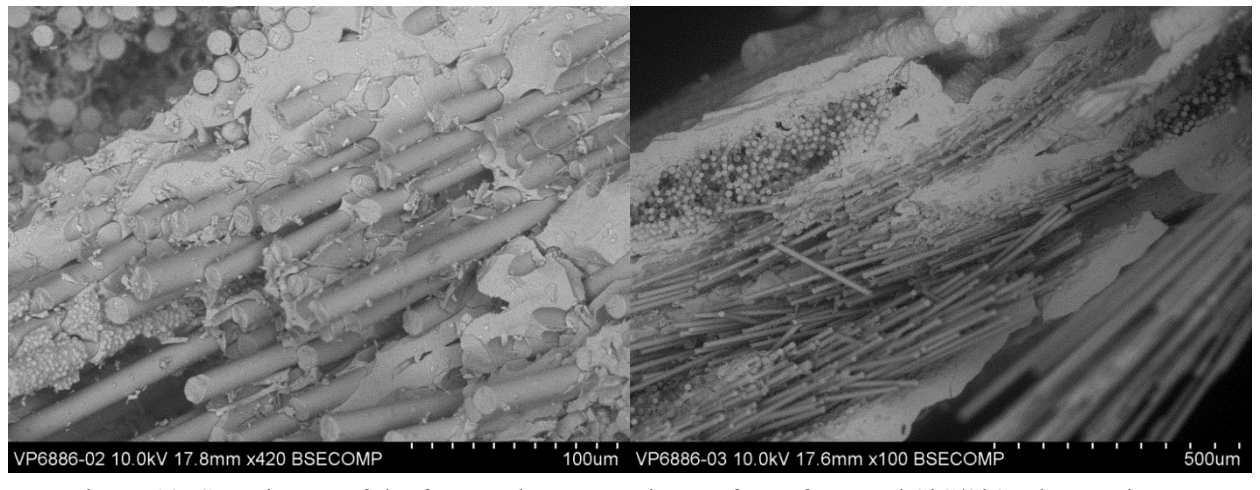


Figure 18: SEM image of the fractured cross-section surface of a tested SiC/SiC tube specimen.

6. SUMMARY

The mechanical properties statistics for nuclear grade SiC/SiC composite tube specimens were evaluated and analyzed. In general, the data show reasonable consistency across the laboratories, indicating that the current C1773-13 ASTM standard is adequate for testing ceramic fiber reinforced ceramic matrix composite tube specimens. The limited statistical variation in the mechanical properties demonstrate that the quality of the SiC/SiC material employed in these tests is appropriate for meeting the nuclear applications requirements regarding the mechanical properties. The ultimate tensile strength data seems to follow the Weibull distribution with shape and scale parameters as 10.1 and 249.1 respectively. The proportional limit strength data fit best with the Lognormal distribution, for the tested material. Precision statistics were calculated based on the round robin data according to the ASTM E691-09 standard, and precision statement was provided.

It was found that the measured dimensions for tube composite specimens vary with different measurement techniques - radiography versus mechanical method of measurement (micrometer, caliper). Therefore, the dimensional measurement technique can significantly influence the measurement of the cross-sectional area and then the calculated mechanical properties. Advanced techniques such as radiography and micro-computed tomography should be preferred over conventional mechanical methods. The work also brought forward the vagueness in the existing method for determining Young's modulus, which can lead to significant variation in the determined values across the laboratories. A method was proposed with the motivation of standardizing the procedure for modulus measurement.

Acknowledgement

The authors would like to thank Charles Shane Hawkins, Don Erdman, Rick Lowden and Chris Stevens from ORNL for their technical support for the mechanical testing. Research work presented herein was conducted at Oak Ridge National Laboratory. Research sponsored by the Advanced Fuels Campaign of the Nuclear Technology R&D program, Office of Nuclear Energy, US Department of Energy, under contract DE-AC05- 00OR22725 with UT-Battelle, LLC. The institutions participating in the inter-laboratory round robin testing campaign, besides Oak Ridge National Laboratory, are acknowledged: General Atomics, United Technology Research Center, Westinghouse – University of Virginia, NASA Glenn Research Center, Southern Research Institute, General Electric – Aviation.

7. REFERENCES

- [1] J. Carmack, F. Goldner, S. M. Bragg-Sitton, and L. L. Snead, "Overview of the US DOE accident tolerant fuel development program," in *Proc. 2013 LWR Fuel Performance Meeting/TopFuel 2013*, 2013, pp. 15-19.
- [2] S. J. Zinkle, K. A. Terrani, J. C. Gehin, L. J. Ott, and L. L. Snead, "Accident tolerant fuels for LWRs: A perspective," *Journal of Nuclear Materials*, vol. 448, pp. 374-379, 2014.
- [3] K. Yueh, D. Carpenter, and H. Feinroth, "Clad in clay," *Nuclear Engineering International*, vol. 55, pp. 14-16, 2010.
- [4] K. Yueh and K. A. Terrani, "Silicon carbide composite for light water reactor fuel assembly applications," *Journal of Nuclear Materials*, vol. 448, pp. 380-388, 2014.
- [5] K. E. Barrett, M. Teague, I. J. Van Rooyen, S. M. Bragg-Sitton, K. Ellis, C. Glass, *et al.*, "Engineering challenges of LWR advanced fuel cladding technology in preparation for in-reactor demonstrations," Oak Ridge National Laboratory (ORNL)2012.
- [6] S. Fazluddin, K. Smit, and J. Slabber, "The use of advanced materials in VHTR's," in *Second International Topical Meeting on High Temperature Reactor Technology*, 2004.
- [7] A. Kohyama, T. Hinoki, T. Mizuno, T. Kunugi, M. Sato, Y. Katoh, *et al.*, "R& D of Advanced material systems for reactor core component of gas cooled fast reactor," in *Proceedings of the International Congress on Advances in Nuclear Power Plants*, 2005, p. 19.
- [8] A. Raffray, R. Jones, G. Aiello, M. Billone, L. Giancarli, H. Golfier, *et al.*, "Design and material issues for high performance SiC f/SiC-based fusion power cores," *Fusion Engineering and Design*, vol. 55, pp. 55-95, 2001.
- [9] N. B. Morley, Y. Katoh, S. Malang, B. A. Pint, A. Raffray, S. Sharafat, *et al.*, "Recent research and development for the dual-coolant blanket concept in the US," *Fusion Engineering and Design*, vol. 83, pp. 920-927, 2008.
- [10] Y. Katoh and K. A. Terrani, "Systematic Technology Evaluation Program for SiC/SiC Composite-based Accident-Tolerant LWR Fuel Cladding and Core Structures: Revision 2015," Oak Ridge National Laboratory (ORNL)2015.
- [11] M. G. Jenkins, E. Lara-Curzio, S. T. Gonczy, and L. P. Zawada, "Multiple-Laboratory Round-Robin Study of the Flexural, Shear, and Tensile Behavior of a Two-Dimensionally Woven NicalonTM/SylramicTM Ceramic Matrix Composite," in *Mechanical, Thermal and Environmental Testing and Performance of Ceramic Composites and Components*, ed: ASTM International, 2000.
- [12] Y. Katoh, K. Ozawa, C. Shih, T. Nozawa, R. J. Shinavski, A. Hasegawa, *et al.*, "Continuous SiC fiber, CVI SiC matrix composites for nuclear applications: Properties and irradiation effects," *Journal of Nuclear Materials*, vol. 448, pp. 448-476, 2014.
- [13] T. Nozawa, K. Ozawa, Y.-B. Choi, A. Kohyama, and H. Tanigawa, "Determination and prediction of axial/off-axial mechanical properties of SiC/SiC composites," *Fusion Engineering and Design*, vol. 87, pp. 803-807, 2012.
- [14] S. W. Tsai and E. M. Wu, "A general theory of strength for anisotropic materials," *Journal of composite materials*, vol. 5, pp. 58-80, 1971.
- [15] E. Rohmer, E. Martin, and C. Lorrette, "Mechanical properties of SiC/SiC braided tubes for fuel cladding," *Journal of Nuclear Materials*, vol. 453, pp. 16-21, 2014.
- [16] C. Deck, G. Jacobsen, J. Sheeder, O. Gutierrez, J. Zhang, J. Stone, *et al.*, "Characterization of SiC–SiC composites for accident tolerant fuel cladding," *Journal of Nuclear Materials*, vol. 466, pp. 667-681, 2015.
- [17] F. Bernachy-Barbe, L. Gélébart, M. Bornert, J. Crépin, and C. Sauder, "Anisotropic damage behavior of SiC/SiC composite tubes: Multiaxial testing and damage

- characterization," *Composites Part A: Applied Science and Manufacturing*, vol. 76, pp. 281-288, 2015.
- [18] Y. Katoh, T. Nozawa, C. Shih, K. Ozawa, T. Koyanagi, W. Porter, *et al.*, "High-dose neutron irradiation of Hi-Nicalon Type S silicon carbide composites. Part 2: Mechanical and physical properties," *Journal of Nuclear Materials*, vol. 462, pp. 450-457, 2015.
- [19] L. Alva, K. Shapovalov, G. M. Jacobsen, C. A. Back, and X. Huang, "Experimental study of thermo-mechanical behavior of SiC composite tubing under high temperature gradient using solid surrogate," *Journal of Nuclear Materials*, vol. 466, pp. 698-711, 2015.
- [20] C. Deck, H. Khalifa, B. Sammuli, T. Hilsabeck, and C. Back, "Fabrication of SiC–SiC composites for fuel cladding in advanced reactor designs," *Progress in Nuclear Energy*, vol. 57, pp. 38-45, 2012.
- [21] J. Zhang, H. Khalifa, C. Deck, J. Sheeder, and C. Back, "Thermal diffusivity measurement of curved samples using the flash method," *Ceramic Materials for Energy Applications V: Ceramic Engineering and Science Proceedings, Volume 36*, p. 43, 2015.
- [22] D. Kim, H.-G. Lee, J. Y. Park, and W.-J. Kim, "Fabrication and measurement of hoop strength of SiC triplex tube for nuclear fuel cladding applications," *Journal of Nuclear Materials*, vol. 458, pp. 29-36, 2015.
- [23] T. Koyanagi, Y. Katoh, K. Ozawa, K. Shimoda, T. Hinoki, and L. L. Snead, "Neutron-irradiation creep of silicon carbide materials beyond the initial transient," *Journal of Nuclear Materials*, vol. 478, pp. 97-111, 2016.
- [24] H. M. Yun and J. A. DiCarlo, "Comparison of the tensile, creep, and rupture strength properties of stoichiometric SiC fibers," in *Proceedings of the 23rd annual conference on composites, materials and structures*, 1999, pp. 259-72.
- [25] A. Urano, J.-i. Sakamoto, M. Takeda, Y. Imai, H. Araki, and T. Noda, "Microstructure and Mechanical Properties of SiC Fiber" Hi-Nicalon Type S" Reinforced SiC Composites," in 22nd Annual Conference on Composites, Advanced Ceramics, Materials, and Structures-A: Ceramic Engineering and Science Proceedings, Volume 19, 2009, p. 55.
- [26] M. Takeda, J. Sakamoto, A. Saeki, and H. Ichikawa, "Mechanical and structural analysis of silicon carbide fiber Hi-Hicalon type S," in *Ceramic Engineering and Science Proceedings*. vol. 17, No. 4, ed Westerville, OH: American Ceramic Society, 1996, pp. 35-42.
- [27] H. Ichikawa, "Polymer-Derived Ceramic Fibers," *Annual Review of Materials Research*, 2016.
- [28] R. J. Kerans, R. S. Hay, T. A. Parthasarathy, and M. K. Cinibulk, "Interface Design for Oxidation-Resistant Ceramic Composites," *Journal of the American Ceramic Society*, vol. 85, pp. 2599-2632, 2002.
- [29] R. Naslain, "Design, preparation and properties of non-oxide CMCs for application in engines and nuclear reactors: an overview," *Composites Science and Technology*, vol. 64, pp. 155-170, 2004.
- [30] T. Noda, H. Araki, H. Suzuki, and F. Abe, "Processing of carbon fiber/SiC composite for low activation," *Materials Transactions, JIM*, vol. 34, pp. 1122-1129, 1993.
- [31] A. Kohyama, "Present status of NITE-SiC/SiC for advanced nuclear energy systems," in 31st International Conference on Advanced Ceramics and Composites, Daytona Beach, 2007.
- [32] T. Koyanagi, K. Ozawa, T. Hinoki, K. Shimoda, and Y. Katoh, "Effects of neutron irradiation on mechanical properties of silicon carbide composites fabricated by nanoinfiltration and transient eutectic-phase process," *Journal of Nuclear Materials*, vol. 448, pp. 478-486, 2014.